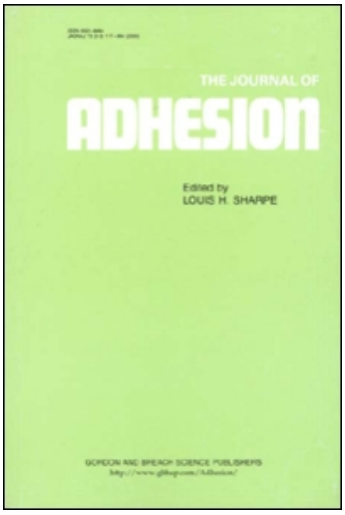

The Journal of Adhesion
Publication details, including instructions for authors and subscription information:
http://www.informaworld.com/smpp/title~content=t713453635

Thermodynamic and Micromechanical Approaches to the Adhesion between Polyethylene Terephthalate and Silicon Oxide

Y. Leterrier[a]; P. Sutter[a]; J. A. E. Månson[a]
[a] Laboratoire de Technologie des Composites et Polymères Ecole Polytechnique Fédérale de Lausanne, Lausanne, Switzerland

To cite this Article Leterrier, Y. , Sutter, P. and Månson, J. A. E.(1999) 'Thermodynamic and Micromechanical Approaches to the Adhesion between Polyethylene Terephthalate and Silicon Oxide', The Journal of Adhesion, 69: 1, 13 — 30
To link to this Article: DOI: 10.1080/00218469908015916
URL: http://dx.doi.org/10.1080/00218469908015916

J. Adhesion, 1999, Vol. 69, pp. 13–30
Reprints available directly from the publisher
Photocopying permitted by license only

Thermodynamic and Micromechanical Approaches to the Adhesion between Polyethylene Terephthalate and Silicon Oxide

Y. LETERRIER, P. SUTTER and J.-A. E. MÅNSON*

Laboratoire de Technologie des Composites et Polymères,
Ecole Polytechnique Fédérale de Lausanne, CH-1015 Lausanne, Switzerland

(Received 27 October 1997; In final form 13 April 1998)

The adhesion between different types of polyethylene terephthalate (PET) substrates coated with thin silicon oxide (SiO_x) layers is examined using two alternative approaches. The surface of the polymer was hydrolyzed or silylated prior to the deposition of the oxide layer, to be compared with untreated PET. The first approach is the thermodynamic adsorption model from which are defined the dispersive and polar components of the polymer surface energy, obtained from wetting measurements. The second approach is the micromechanical analysis of the interface stress transfer which provides the interface shear strength from the measurement of the density of coating cracks *vs.* applied tensile strain. The hydrolysis treatment slightly hydrophobizes the PET surface; however, it does not significantly modify the interface shear strength compared with the untreated material. By contrast, the silane treatment improves the polar component of the PET, which is related, to a first approximation, to the measured 30% increase of the interface shear strength compared to the untreated material.

Keywords: Polyethylene terephthalate; silicon oxide; hydrolysis; silylation; interface shear strength; dispersive interaction; polar interaction

1. INTRODUCTION

Silicon oxide coated polymers have found large interest for food and pharmaceutical packaging industries [1–3], thanks to recent progress

*Corresponding author. Tel: +41 21 693 4281/4285, Fax: +41 21 693 5880, e-mail: leterrier@epfl.ch

in the development of plasma-assisted deposition techniques [4]. These oxygen-barrier materials exhibit excellent tolerance for the thermo-mechanical stresses encountered during the various conversion processes present during manufacture of the package. In the fabrication process, films are subjected to several heating and cooling cycles as, for instance, during lamination and welding with other polymer films, or during subsequent sterilization. These operations introduce complex internal stress states in the different layers, and might also change the structure of the semi-crystalline polymers [5]. Moreover, folding of the multilayer film strains the material at strain rates as high as several s^{-1}. In these operations, the limiting factor is the durability of the oxide barrier layer: it must not crack or detach from the substrate. A crack in the oxide layer does not by itself deteriorate significantly the barrier performance, providing that the substrate is not strained beyond approximately 3% strain [5]. Cracks are primarily controlled by the cohesion of the oxide material. The cohesion depends obviously on the deposition conditions [6, 7]; it is higher when the oxide layer is thinner, and is improved through the introduction of compressive stresses, either during deposition [8], or with appropriate annealing treatments [5]. Conversely, the delamination of the layer opens a large window for oxygen penetration and should, therefore, be avoided. Delamination is controlled by interfacial adhesion. Recent works have shown that the interfacial shear strength in SiO_x/PET films in comparable with, or even slightly higher than, the bulk shear stress of the polymer substrate, thanks to the strain hardening of the PET in the plastic regime [5]. Combined with ToF-SIMS analyses that showed that failure occurs at the interface, and is of adhesive nature [9], this result indicates that the adhesive strength of the interface is as high as the cohesive strength of the polymer substrate. Nevertheless, delamination was detected in the form of tent-shaped areas when the film was loaded in compression. Therefore, a need exists to improve further the adhesion of the oxide layer to the PET substrate.

A considerable number of technological applications use polymers in intimate contact with other materials, ranging from paints and coatings to composites. It is well established that the reliability of such applications depends directly upon the adhesion between the different materials; the interest in durability of interfaces keeps on increasing as seen from the increasing body of literature and number of conferences

on the topic (*e.g.*, Refs. [10, 11]). The mechanisms of adhesion between a polymer and another material have been extensively stuided, although only partially elucidated. Among the reasons for this lies the variety of polymer structures and material combinations, and of bonding procedures, resulting in a multiplicity of interface structures and stress states. As a consequence, a large number of adhesion theories and adhesion measurement methods have emerged since the early 30's and have been reviewed by several authors [12–17]. According to Mittal [15], the most appropriate adhesion measurement method is the one that simulates stress conditions achieved during service. This principle is at the base of the development of several quantitative methods developed together with a mechanical description of the interface stress transfer, to model the test results [18, 19]. However, the practical dimensions and geometry of the manufactured product together with the often very complex arrangement of the various material phases, such as in fiber-reinforced composite parts, prohibit a direct and comprehensive characterization of interfacial adhesion. Nevertheless, most of the recent techniques have proven to be useful to determine the effect of specific treatments on adhesion performance. Adhesion test methods either introduce a third body to stress the interface or use model specimens to apply thermal or mechanical loads to the interface without the need for a third body. The former, developed mainly to assess coating adhesion, include the tape and similar pull-off methods, and the scratch and indentation tests, which do not necessarily reflect the buried character of the interface. The latter type of adhesion methods often use model specimens, among which the single fiber fragmentation test has been extensively analyzed [19–27]. One drawback with such test is that the manufacture of the specimens inevitably generates inhomogeneous interfacial structures and internal stress, resulting from polymer flow and thermal and pressure gradients. The influence of such factors on adhesion is *a priori* unknown, although it is recognised that it can be considerable [19, 27], following, for instance, analyses of stress birefringence patterns in the interface vicinity, and of strain fields by means of Raman Spectroscopy [26, 27].

A refined understanding of the macroscopic properties such as adhesion is gained from the analysis of the physico-chemical interactions involved in adhesion mechanisms. An interesting route

has been shown to be the thermodynamic adsorption model of Sharpe and Schonhorn [28]. This alternative and complementary approach to the mechanical characterizations described above is now widely used, in the case of an intimate contact between the polymer and the second phase, where adhesion results from intermolecular interactions acting on short distances in the order of several Å. In this sense, adhesion is achieved through wetting of one substance onto the other, and related theories originate from the works of Young [29] and Dupré [30] which introduce surface energy characteristics of both substances and define the reversible work of adhesion. Generalisations to the case of solids expressed the surface energy as a function of the various dispersive and non-dispersive interactions. Whereas the contribution of the dispersive, or Lifshitz-van der Waals, components to the work of adhesion between the two materials appears to be well at hand [31, 32], the contribution of the non-dispersive components is less clear. Numerous interactions are indeed of non-dispersive nature; these include dipolar interactions, hydrogen bonds and other acid-base interactions, and interactions related to metallic bonds [33]. In the case of polymers, it has further been established that the molecular surface structure, mainly segmental orientation, could be affected by the presence of the substance wetting onto it (*e.g.*, Ref. [34]). Nevertheless, as shown initially by Fowkes *et al.* [35, 36], the acid-base interaction could contribute significantly to the overall adhesion.

An interesting correlation between mechanical properties and interfacial interactions was developed by Nardin and Schultz in the early 90's [37–40] for a variety of fiber-reinforced polymer composites. In these materials, the fibers are embedded within the polymer matrix and processed together according to an appropriate pressure and temperature cycle to the desired product. In a recent study devoted to thin coatings evaporated on a polymer film [41], *i.e.*, where the processing conditions differ substantially from the fiber composite case, the work of adhesion between polyethylene terephthalate (PET) and silicon oxide, calculated from stress transfer mechanics combined with the above approach, was found to be close to 230 mJ/m^2. This value was in good agreement with the estimated work of adhesion at the SiO_2/PMMA interface [42]. This was a good indication that strong specific interactions were involved, such as hydrogen bonds, established between silanol groups of the oxide and oxygen-containing

carboxyl groups of the polymer, which nearly double the work of adhesion of basic polymers to silica [42]. However, in the present situation, the nature of the plasma deposition process together with the resulting covalent bonds prohibits the calculation of the work of adhesion from the surface tensions of the interacting substances.

The aim of this study was to use alternative approaches to characterize the adhesion in the case of oxide coatings processed by means of plasma-enhanced chemical vapor deposition onto PET. First is the measure of the dispersive and polar contribution to the polymer surface energy and second is the micromechanical modelling of the stress-transfer at the interface. For this purpose, various PET surfaces were prepared by means of hydrolysis and silylation, and these controlled surfaces were coated with the oxide under identical deposition conditions. Correlatively, a second objective of the study was to investigate the effect of the treatments of the PET surface prior to the deposition of the oxide coating on both its cohesion and adhesion to the polymer. Hydrolysis, through an increase of the number of hydroxyl sites [43], was expected to promote interactions with silicon oxide. Silylation with appropriate functional silanes, developed several decades ago to improve interfacial interactions between polymers and glass surfaces [44, 45], was also foreseen to improve the adhesion between the polymer and the coating.

2. EXPERIMENTAL SECTION

2.1. The PET Substrate and the Surface Treatments

A PET copolymer of $M_w = 63{,}500$ daltons and polydispersity close to 2.5 was used (Eastman Chemical 9921 W). The PET substrate was injection molded from pellets into 1 mm thick square plaques ($50 \times 50\,mm^2$), subsequently machined carefully into dog-bone tensile test specimens. Prior to the deposition process of the oxide layer, the PET was subjected to two different surface treatments. The Young's modulus of the PET substrate was measured from tensile tests performed at room temperature at constant strain rate of $4.8 \times 10^{-5}\,s^{-1}$ on a UTS machine. It was found to be independent of the surface treatments and equal to 2500 ± 30 MPa. The first treatment was the

hydrolysis of the PET surface in a sodium hydroxide solution ($c = 2\,M$) during 20 min at 60°C [43]. The second treatment was the silylation of the PET surface in a γ-aminopropyltriethoxysilane (γ-APS, OSi Specialities A1100) during 10 min at 60°C. The silane possesses two terminal groups with different chemical reactivities. It was, therefore, expected that the primary amino end-group would condense with the polymer and that the alkoxy end-group would react after hydrolysis with the silanol functions of the oxide. The untreated samples were rinsed with ethanol, and the hydrolyzed and silane-treated were immersed in a hexane solution in a ultrasonic bath during 5 min, to clean the PET surface prior to the deposition. Contact angle measurements were carried out at room temperature with demineralized water and apolar α-bromonaphtalene to characterize the influence of the two treatments on the surface properties of the substrate. Contact angles were calculated by measuring the height, h_{drop}, and diameter, d_{drop}, of the liquid drop deposited on the substrate by means of a binocular macroscope (Olympus SZH). When gravity effects are negligible, *i.e.*, low Bond number values, the contact angle is independent of the drop volume and is given by $\theta = 2\arctan(2h_{drop}/d_{drop})$ [46].

2.2. Deposition of the Oxide Layer

The coating deposition was done using plasma-enhanced chemical vapor deposition (PECVD), originally developed by Airco Coating Technology (CA, USA) [2, 3]. The method has been widely used in the semiconductor industry in the fabrication SiO_2 and Si_3N_4 layers on microprocessors. In the deposition process, the PET substrate was mounted in the deposition chamber under 0.1 mbar. The silane source was hexamethyldisiloxane, pumped into the chamber together with oxygen and argon. The resulting SiO_x stoichiometry was $x = 1.8-1.9$. The coating thickness was measured by X-ray fluorescence and found equal to 120 ± 3 nm. The Young's modulus of the oxide coating was assumed to be equal to 79.5 GPa. This value had been measured for a $SiO_{1.7}$ oxide coating, whose modulus was deduced from tensile tests carried out on coated and uncoated PET films by applying the rule of mixtures [5].

2.3. Fragmentation Testing and Morphological Analysis

In the fragmentation test, coated PET samples were loaded in tension and the resulting fragmentation of the coating was recorded as a function of applied strain, as detailed in Ref. [5]. The fragmentation tests were performed at room temperature at a constant strain rate of $4.8 \times 10^{-5}\,s^{-1}$ on a Minimat Miniature Materials Tester (Rheometrics). The equipment was mounted under an optical microscope (Olympus SH-2), to measure the increase in crack density (CD) as a function of applied strain until fragmentation saturation, where CD becomes constant. The morphology of the fragmented SiO_x coating was further analyzed from scanning electron micrograph (SEM) of samples strained beyond the saturation onset strain. In order to overcome charging effects on the SiO_x surface, all samples were coated with a thin gold layer. The JEOL JSM 6300 SEM was operated at 3 kV.

3. EXPERIMENTAL RESULTS

3.1. Wetting Measurements

Contact angles of demineralized water and α-bromonaphtalene measured on the different surfaces are reported in Table I. The relatively large error on several measurements might be related to the presence of polar impurities at the surface, as the cleaning with hexane only dissolves non-polar impurities. A polar solvent such as acetonitrile should alleviate this problem. A significant increase in contact angles with water is, nevertheless, noticed after the hydrolysis treatment. The corresponding increase in hydrophobicity is surprising: such treatment was, on the contrary, expected to increase the degree of

TABLE I Contact angles of water and α-bromonaphtalene on various PET surfaces

Surface type	*Contact angle (degrees)*	
	water	*α-bromonaphtalene*
Untreated PET	69.5 ± 0.3	32.0 ± 2.0
Hydrolyzed PET	77.0 ± 1.4	17.2 ± 0.1
Silylated PET	63.8 ± 2.6	32.5 ± 0.5

interactions with water through an increased accessability of carboxyl and hydroxyl groups [43]. Among possible explanations one may consider molecular weight degradation which would have overcome the increased accessibility of hydroxyl sites, or the presence of hexane residues; a more detailed examination is needed at this point. The decrease in contact angle with apolar α-bromonaphtalene reveals the enhanced non-polar characteristics of the hydrolyzed surface. On the contrary, it is observed that the silylation affects only the polar character of the modified PET surface, which becomes more hydrophilic.

3.2. Fragmentation of the Oxide Layer on PET Substrates

Figure 1 shows the morphology of the fragmented oxide on the untreated PET substrate, strained beyond the saturation onset strain. At this stage, primary cracks [5], parallel to the tensile direction, are largely open and leave wide PET areas visible underneath [9]. In these

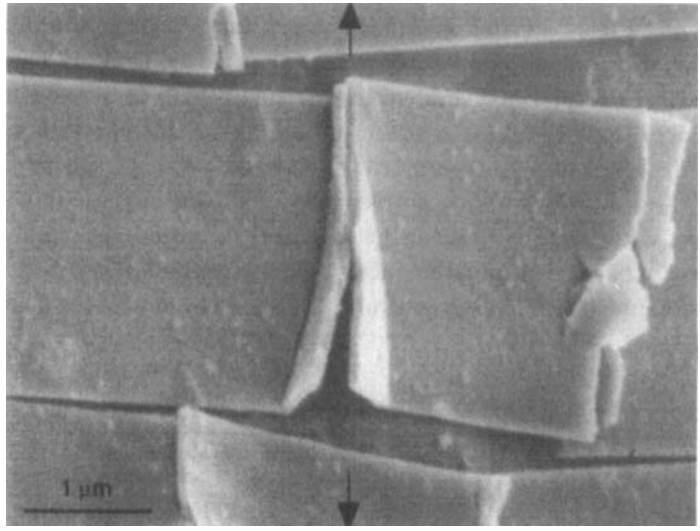

FIGURE 1 Morphology of the SiO_x coating on the untreated PET substrate strained beyond the onset strain for the coating fragmentation saturation. Delamination is evident under the tent-shaped buckle. The arrows indicate the loading direction.

areas, no particular polymer fibrillation is evident. Secondary cracks, initiated around 10% strain as a result of Poisson's ratio compression effects [5, 41], also appear in the form of tent-shaped buckles. The oxide fragments are partially delaminated from the PET substrate; detachement is even total under the edges of the tents [8]. A very similar morphology was observed in the case of the hydrolyzed material. On the contrary, as shown in Figure 2 for the silylated material, buckling failures of the oxide do not form tents that detach from the substrate, as was observed in Figure 1. Further, a large amount of polymer fibrillation is visible at the surface of the substrate in between two adjacent fragments. These observations are a strong evidence that the coating adhesion has been improved by the silane treatment.

4. DISCUSSION

The deposition processes of thin films on polymers are known to promote intimate contact between the two substances, resulting in a

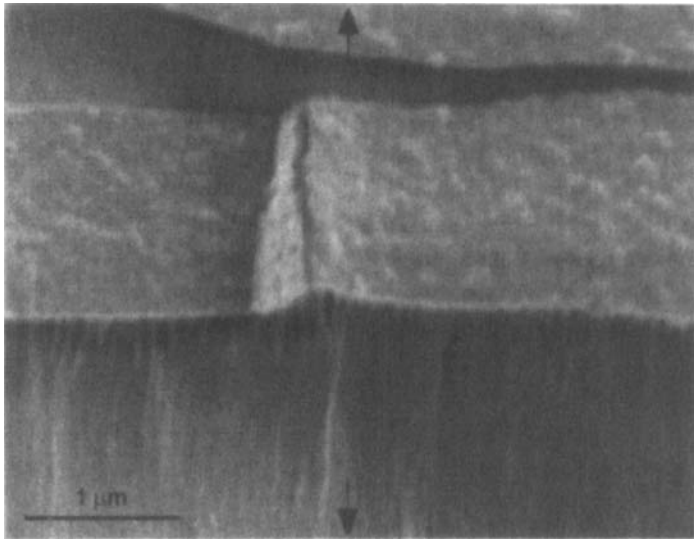

FIGURE 2 Morphology of the SiO_x coating on the silylated PET substrate strained beyond the onset strain for the coating fragmentation saturation. Polymer fibrillation is evident between adjacent fragments. The arrows indicate the loading direction.

high density of short distance intermolecular interactions. Such intimate contact implies no interfacial defects, *i.e.*, perfect wetting [47]. The plasma process is indeed known to promote chemical bonds, typically Si—O—C and Si—C in the case of SiO_x on PET [48]. The presence of such interactions together with the simultaneous etching of the polymer and deposition of the plasma coating prohibits the calculation of the work of adhesion from the wetting theory developed by Sharpe and Shornhorn [28]. The derivation of the dispersive and polar components of the polymer surface is, nevertheless, possible and interesting, as these relate to the interface formation and, ultimately, to the interface strength [48, 49]. Moreover, as only limited delamination was found to occur, even at high applied strains, stress transfer models are likely to be best applied to assess the interface shear strength [41]. These two independent approaches – thermodynamics and micromechanics – stemming from the wetting measurements and the fragmentation tests described previously were compared to identify the influence of the treatments investigated. It was anticipated that this comparison would provide an insight into the nature of interface interactions between PET and SiO_x.

4.1. The Polar Contribution to the PET Surface Energy

The surface energy of the polymer, γ_{PET}, is the sum of a dispersive component (London interactions), γ^d_{PET}, and a non-dispersive component (polar interactions, including acid-base interactions such as hydrogen bonds), γ^{nd}_{PET}. Each component was derived from the measurements of contact angles θ of the selected liquids of known surface energy characteristics, α-bromonaphtalene being apolar with $\gamma^{nd} = 0$, through the following expression [33]:

$$\cos\theta + 1 \approx 2\left[\frac{\sqrt{\gamma^d_{PET}\gamma^d_{liq}}}{\gamma_{liq}} + \frac{\sqrt{\gamma^{nd}_{PET}\gamma^{nd}_{liq}}}{\gamma_{liq}}\right] \quad (1)$$

where the subscript liq refers to the selected liquid. In a plot of $\cos\theta$ *vs.* $\sqrt{\gamma^d_{liq}}/\gamma_{liq}$, it has been observed that apolar liquids including α-bromonaphtalene lie on a straight line of slope $2\sqrt{\gamma^d_{PET}}$ and intercept

-1. The value of $\sqrt{\gamma_{PET}^{nd}\gamma_{liq}^{nd}}/\gamma_{liq}$, hence of γ_{PET}^{nd}, is inferred from the difference between the ordinates of the point corresponding to water and of the point with the same absissa as water on the straight line. The surface energy components of the modified PET surfaces reported in Table II are comparable with those found in others works ($\gamma_{PET}^{d} = 36.5 - 43.2\,mJ/m^2$ and $\gamma_{PET} = 41.3 - 49.5\,mJ/m^2$ [50–54]). As previously pointed out for the wetting measurements, the results indicate that the hydrolysis of the PET surface slightly increases the dispersive component of the polymer surface tension, whereas it decreases the polar component, although the surface tensions of the untreated and hydrolyzed polymers are found to be almost identical. Effects are opposite in the case of silane treatment, which results in an increase in the polar component of surface tension.

4.2. Micromechanical Approach to the PET/SiO_x Adhesion

The interface shear strength, τ, was derived from the classical Kelly–Tyson model of stress transfer [57, 58]:

$$\tau = 1.337 \cdot h \frac{\sigma_{max}(l_c)}{\bar{l}_{sat}} \tag{2}$$

where h is the coating thickness, σ_{max} is the coating strength at critical length l_c, and $\bar{l}_{sat}$ is the average fragment size at saturation, directly measured from micrographs of fragmented specimens above the saturation onset strain. All the parameters of the RHS in Eq. (2) are known from direct measurements with the exception of l_c and σ_{max}.

The critical length, l_c, was calculated to be very close to $3/2 \cdot \bar{l}_{sat}$ [41, 59] providing that no delamination is present at saturation. It was

TABLE II Surface and interface characteristics of PET/SiO_x systems

Surface type	*Dispersive interaction, γ^d (mJ/m^2)*	*Non-dispersive interaction, γ^{nd} (mJ/m^2)*	*Surface energy, γ (mJ/m^2)*
Water [55]	21.8 ± 0.7	51	72.8
α-bromonaphtalene [56]	47 ± 7	≈ 0	44.6
Untreated PET	38.8	7.9	46.7
Hydrolyzed PET	42.7	3.9	46.6
Silylated PET	37.9	11.0	48.9

further assumed that this relation between l_c and $\bar{l}_{sat}$ was valid even in the presence of limited delamination, which nevertheless induces a negligible error [60]. This applicability of such a one-dimensional model has already been established for similar materials; one argument is that the fragment length distributions at saturation are very narrow and are reasonably well fitted by the theoretical distributions calculated from the Kelly–Tyson assumptions, assuming a stochastic fragmentation process [41]. The experimental and theoretical distributions of fragment lengths at saturation are shown in Figure 3 for the untreated and treated PET/SiO_x materials. For such histograms, around 100 individual fragments, delimited by two primary cracks, have been measured from several micrographs taken on arbitrary locations across the specimen. The calculated oxide critical length, l_c, is reported in the histograms [24]. In each instance, it is evident that the fragmentation distributions are relatively narrow and not far from falling between l_c and $l_c/2$. In particular, less than 8% of the fragments are larger than the calculated value of the critical length, whatever the treatment of the PET substrate. Besides, the broadening of the distribution to smaller lengths has been discussed in

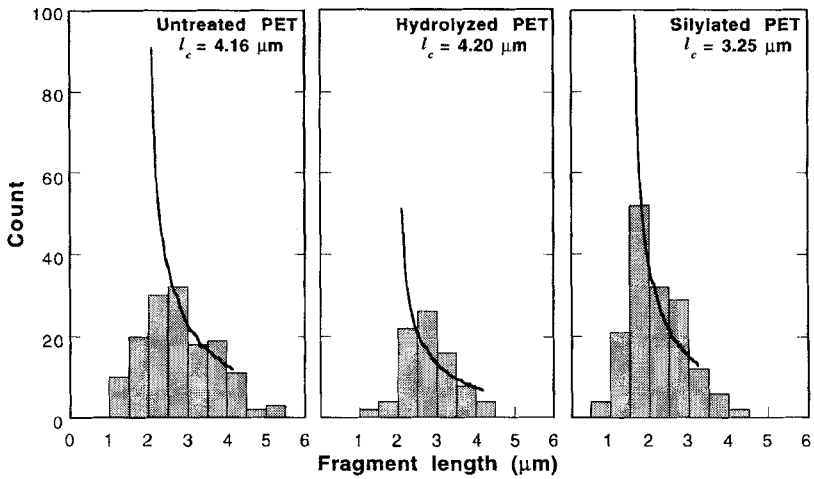

FIGURE 3 Effect of the PET surface treatment on experimental (bars) and theoretical (lines) SiO_x fragment length distributions at saturation; critical fragment lengths are also indicated.

recent work [5]. The critical lengths of untreated and hydrolyzed materials can be considered to be equal, the difference being less than 1%, which is well below the typical uncertainty of the order of 10% related to such measurement [5]. For these materials, the theoretical distribution matches the experimental data for the large fragments, whereas it overestimates the amount of small fragments. This discrepancy reflects the presence of moderate delamination. Conversely, the fragment length distribution of the silylated material is shifted to smaller lengths, its theoretical fit is better, and the corresponding critical length is much lower than that of the two other materials. This latter result confirms the observation of negligible delamination, that is, improved adhesion shown in Figure 2, as smaller critical lengths result from higher adhesion [22].

The dependence of the oxide strength, σ_{max}, with fragment length was calculated from a linear extrapolation of the initial part of the curve Ln{CD} *vs.* Ln{ε}, where ε is the nominal strain, assuming a two-parameter (α and β) Weibull distribution [61–63]:

$$\sigma_{max}(l) = \beta \cdot (l/l_0)^{-1/\alpha} \cdot \Gamma\{1 + 1/\alpha\} \tag{3}$$

where the normalizing factor $l_0 = 1\,\mu m$ and Γ is the gamma function.

The Weibull parameters α and β and the resulting values of σ_{max} and τ, including measured values of the crack onset strain, are reported in Table III for the three types of materials. Whereas the Weibull parameters differ significantly between the hydrolyzed material and the two others, it is found that the surface treatments affect neither the crack onset strain nor the strength of the oxide, within experimental uncertainties. The reason for such large differences in the Weibull parameters is not clear, although it might come

TABLE III Crack onset strain, Weibull parameters, cohesive strength and interface shear strength of SiO_x on various PET substrates

Surface type	*Crack onset strain (%)*	α	β *(MPa)*	SiO_x *strength,* σ_{max} *(MPa)*	*Interface strength,* τ *(MPa)*
Untreated PET	1.30 ± 0.20	6.70	1938	1460 ± 300	87 ± 11
Hydrolyzed PET	1.30 ± 0.20	2.64	3102	1600 ± 320	86 ± 8
Silylated PET	1.15 ± 0.20	6.04	1858	1420 ± 280	112 ± 12

from the experimental difficulty in obtaining sufficient data in the crack-onset regime. In the following, an average value, $\sigma_{max} = 1500$ MPa, will be used. Interestingly, this value is comparable with the strength of PVD (physical vapor deposition) coatings of similar thicknesses [64]. The interface shear strengths between SiO_x and untreated or hydrolyzed PET are found to be almost identical, in inverse proportion to their respective critical lengths also found to be very close to one another, the critical length of the silylated material being 22% smaller than that of the untreated material, and the interface strength of the former being 28% higher than that of the latter. The silylated interface is stronger than the others, which confirms the observations from the SEM micrographs reported earlier. Adhesion is high enough between the silylated surface and the oxide to prevent delamination from taking place and, therefore, all the interface strain concentrates between adjacent coating fragments.

4.3. The Role and Nature of the Interfacial Interactions

Typical interactions between PET and SiO_x obtained by PECVD involve C—Si and C—O—Si chemical bonds [47, 48] and, most likely, hydrogen-bonding interactions established between silanols groups of the oxide and the carboxylic functions of the polymer, whose acid-base character is known to increase considerably the work of adhesion between basic-type polymers and silicon oxide [42]. Hydrolysis of PET surface prior to the deposition of the oxide was found to decrease the work of adhesion. It is probable that the corresponding molecular weight degradation has overcome the increased accessibility of hydroxyl sites; a more detailed examination is needed at this point. Silylation was, on the contrary, particularly efficient regarding adhesion improvement. The 30% increase of the interface shear strength compared with the untreated material indicates that silylation promotes further intimate contact in the earlier stages of the deposition process. The corresponding presence of a large density of hydroxyl sites at the silylated PET surface would, therefore, increase interactions with the growing silicon oxide layer, probably through Si—O—Si bonds together with hydrogen bonds. As shown in Figure 4, and to a first approximation, increase of the

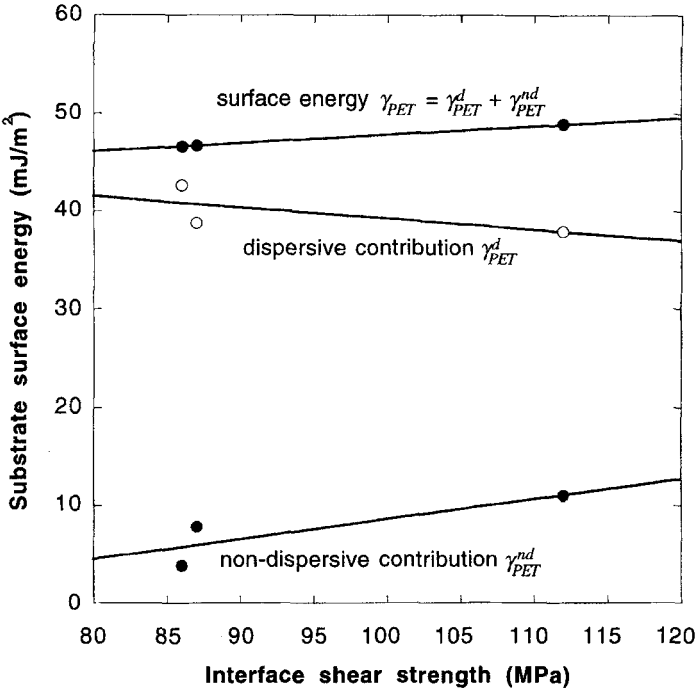

FIGURE 4 PET/SiO_x interface shear strength *vs.* PET surface energy, sum of the dispersive and non-dispersive components determined prior to the deposition of the oxide layer. The lines are an aid to the eye to suggest that correlations exist between the final interface properties and the initial surface characteristics of the polymer substrate.

interface shear strength relates to an increase of the polar component of the surface energy of the polymer substrate. This observation agrees qualitatively with several studies dealing with plasma modifications of several polymer surfaces (*e.g.*, Refs. [47–49]). Obviously, this correlation does not account for the covalent interactions mentioned previously, and a detailed investigation of the chemical structure of the PET/SiO_x interface resulting from the plasma process is required. A promising approach would be to analyze the nature of the surface opened between adjacent fragments as those observed in Figures 1 and 2. To this end, chemical information obtained by ToF-SIMS imaging proved its usefulness in the case of sputtered oxide layers [9], and further allowed to identify the locus of failure.

5. CONCLUSIONS

The adhesion between several polyethylene terephthalate (PET) injection molded substrates and thin silicon oxide (SiO_x) coatings obtained by plasma-enhanced chemical vapor deposition was investigated. The surface of the polymer was hydrolyzed or silylated prior to the deposition of the oxide, and the corresponding dispersive and polar contributions to the surface energy were derived from wetting measurements with a pair of liquids, one being apolar. The adhesion of the oxide layer to the polymer was derived from a micromechanical analysis of the interface stress transfer. In this approach, the interface shear strength was related to the coating tensile strength and the density of coating cracks resulting from straining the coated polymer in uniaxial tension.

The fragmentation pattern of the oxide layer on the untreated PET strained beyond the fragmentation saturation onset was characterized by moderate delamination in the form of tent-shaped buckling failures clearly detached from the polymer. The corresponding interface shear strength was found equal to 87 MPa. Hydrolysis was found to hydrophobize slightly, and most likely degrade, the polymer surface; however, the critical stress transfer length and interface shear strength were found equal to those of the untreated material.

On the contrary, silylation improved the polar character of the PET surface. The fragmented morphology was characterized by large polymer fibrillation in between adjacent oxide fragments. The critical length was found to be smaller than that calculated for the untreated and hydrolyzed PET, corresponding to a 30% increase of the interface shear strength. These observations and measures all demonstrate improved adhesion, which could be related, to a first approximation, to the enhanced polar character of the polymer surface.

Acknowledgements

The authors are gratefully indebted to the Swiss National Science Foundation for funding this work, and to the Centre Interdépartemental de Microscopie Electronique (CIME) of the Ecole Polytechnique Fédérale de Lausanne (EPFL) for the SEM support. They

acknowledge P. Fayet of TetraPak Suisse for the preparation of the oxide coatings.

References

[1] Brody, A. L., In: *Proc. Micro-ready Foods'88* (1988).
[2] Felts, J. T. and Grubb, A. D., *J. Vac. Sci. Technol.* **A10**, 1675 (1992).
[3] Felts, J. T., *J. Plastic Films and Sheeting* **9**, 201 (1993).
[4] Yasuda, H., *Plasma Polymerisation* (Academic Press, New York, 1985).
[5] Leterrier, Y., Boogh, L., Andersons, J. and Månson, J.-A. E., *J. Polym. Sci. B: Polym. Phys.* **35**, 1449 (1997).
[6] Candron, E., Band, G., Besse, J. P., Blondiaux, G. and Jacquet, M., *Solid State Ionics* **70/71**, 629 (1994).
[7] Marechal, N., Quesnel, E. and Parleau, Y., *Thin Solid Films* **241**, 34 (1994).
[8] Rosenberg, M., *Diploma work* EPFL-LTC, Switzerland (1996).
[9] Pitton, Y., Hamm, S. D., Lang, F.-R., Mathieu, H. J., Leterrier, Y. and Månson, J.-A. E., *J. Adhesion Sci. Technol.* **10**, 1047 (1996).
[10] *Controlled Interphases in Composite Materials*, Ishida, H., Ed. (Elsevier, New York, 1990).
[11] *Progress in Durability Analysis of Composite Systems*, Cardon, A. H., Fukuda, H. and Reifsnider, K. A. A., Eds. (Balkema Publishers, Rotterdam, 1996).
[12] Mittal, K. L., *Electrocomp. Sci. Technol.* **3**, 21–42 (1976).
[13] *Adhesion Measurement of Thin Films, Thick Films, and Bulk Coatings*, Mittal, K. L., Ed. (ASTM, Philadelphia, 1978).
[14] Valli, J., *J. Vac. Sci. Technol.* **A4**, 3007 (1986).
[15] Mittal, K. L., *J. Adhesion Sci. Technol.* **1**, 247 (1987).
[16] Drzal, L. T. and Madhukar, M., *J. Mater. Sci.* **28**, 569 (1990).
[17] *Adhesion Measurement of Films and Coatings*, Mittal, K. L., Ed. (VSP, Utrecht, 1995).
[18] Steinmann, P. A. and Hintermann, H. E., *J. Vac. Sci. Technol.* **A7**, 2267 (1989).
[19] Pitkethly, M. J., Favre, J. P., Gaur, U., Jakubowski, J., Mudrich, S. F., Caldwell, D. L., Drzal, L. T., Nardin, M., Wagner, H. D., Dilandro, L., Hampe, A., Armistead, J. P., Desaeger, M. and Verpoest, I., *Compos. Sci. Technol.* **48**, 205 (1993).
[20] Wagner, H. D. and Eitan, A., *Appl. Phys. Lett.* **56**, 1965 (1990).
[21] Curtin, W. A., *J. Mater. Sci.* **26**, 5239 (1991).
[22] Monette, L., Anderson, M. P. and Grest, G. S., *Polym. Compos.* **14**, 101 (1993).
[23] Feillard, P., Désarmot, G. and Favre, J. P., *Compos. Sci. Technol.* **49**, 109 (1993).
[24] Feillard, P., Désarmot, G. and Favre, J. P., *Compos. Sci. Technol.* **50**, 265 (1994).
[25] Lacroix, T., Keunigs, R., Desaeger, M. and Verpoest, I., *J. Mater. Sci.* **30**, 683 (1995).
[26] Huang, Y. and Young, R. J., *Compos. Sci. Technol.* **52**, 505 (1994).
[27] Andrews, M. C., Bannister, D. J. and Young, R. J., *J. Mater. Sci.* **31**, 3893 (1996).
[28] Sharpe, L. H. and schonhorn, H., *Chem. Eng. News.* **15**, 67 (1963).
[29] Young, T., *Phil. Trans. Roy. Soc. London* **95**, 65 (1805).
[30] Dupré, A., Théorie mécanique de la chaleur (Gauthier-Villars, Paris, 1869), p. 393.
[31] Girifalco, L. A. and Good, R. J., *J. Chem. Phys.* **61**, 904 (1957).
[32] Fowkes, F. M., *Ind. Eng. Chem.* **56**, 40 (1964).
[33] Fourche, G., *Polym. Eng. Sci.* **35**, 957 (1995).
[34] Lavielle, L. and Schultz, J., *J. Coll. Interface Sci.* **106**, 438 (1985).
[35] Fowkes, F. M. and Mostafa, M. A., *Ind. Eng. Chem. Proc. Res. Dev.* **17**, 3 (1978).
[36] Fowkes, F. M., *J. Adhesion Sci. Technol.* **1**, 7 (1987).

[37] Schultz, J. and Nardin, M., In: *Controlled Interphases in Composite Materials* Ishida, H., Ed. (Elsevier, New York, 1990), p. 561.
[38] Nardin, M., Asloun, E. M. and Schultz, J., *Polym. Adv. Technol.* **2**, 115 (1991).
[39] Nardin, M. and Schultz, J., *Compos. Interfaces* **1**, 177–192 (1993).
[40] Nardin, M. and Schultz, J., *Langmuir* **12**, 4238 (1996).
[41] Leterrier, Y., Wyser, Y., Månson, J.-A. E. and Hilborn, J., *J. Adhesion* **44**, 213 (1994).
[42] Fowkes, F. M., Dwight, D. W., Cole, D. A. and Huang, T. C., *J. Non-Cryst. Sol.* **120**, 47 (1990).
[43] Zeronian, S. H., Wang, H.-Z. and Alger, K. W., *J. Appl. Polym. Sci.* **41**, 527 (1990).
[44] Plueddemann, E. P., *Silane Coupling Agents* (Plenum Press, New York, 1982).
[45] Ishida, H., In: *The Interfacial Interactions in Polymeric Composites*, Akovali, G., Ed. (Kluwer Academic Publishers, London, 1993).
[46] Walliser, A., *Ph. D. Thesis*, Université de Haute Alsace, France, 92-MULH-0248 (1992).
[47] Rotger, J. C., Pireaux, J. J., Caudano, R., Thorne, N. A., Dunlop, H. M. and Benmalek, M., *J. Vac. Sci. Technol.* **A13**, 260 (1995).
[48] Benmalek, M. and Dunlop, H. M., *Surf. Coatings Technol.* **76–77**, 821 (1995).
[49] Garby, L., Chabert, B., Sage, D., Soulier, J. P. and Bosmans, R., *Angew. Makromol. Chem.* **210**, 21 (1993).
[50] Owens, D. K. and Wendt, R. C., *J. Appl. Polym. Sci.* **13**, 1741 (1969).
[51] Wu, S., *J. Phys. Chem.* **72**, 3332 (1968).
[52] Dann, J. R., *J. Coll. Interface Sci.* **32**, 302 (1970).
[53] Wu, S., In: *Adhesion and Adsorption of Polymers*, Lee, L.-H., Ed. (Plenum Press, New York, 1980).
[54] Anhang, J. and Gray, D. G., In: *Physicochemical Aspects of Polymer Surfaces*. vol. 2, Mittal, K. L., Ed. (Plenum Press, New York, 1983), 664
[55] Van Oss, C. J., Chaudhury, M. K. and Good, R. J., *Adv. Coll. Interf. Sci.* **28**, 35 (1987).
[56] van Oss, C. J., In: *Polymer Surfaces and Interfaces II*, Feast, W. J., Munro, H. S. and Richards, R. W. Eds. (John Wiley and Sons, New York 1993), Chap. 11.
[57] Kelly, A. and Tyson, W. R., *J. Mech. Phys. Sol.* **13**, 329 (1965).
[58] Hu, M. S. and Evans, A. G., *Acta Metall.* **37**, 917 (1989).
[59] Kimber, A. C. and Keer, J. G., *J. Mater. Sci. Letters* **1**, 353 (1983).
[60] Leterrier, Y. and Månson, J.-A. E., *J. Mater. Sci. Letters* **16**, 120 (1997).
[61] Yavin, B., Gallis, H. E., Scherf, J., Eitan, A. and Wagner, H. D., *Polym. Compos.* **12**, 436 (1991).
[62] Andersons, J., Joffe, R. and Sandmark, R., *Mech. Compos. Mater.* **31**, 35 (1995).
[63] Weibull, W., *J. Appl. Mech.* **18**, 293 (1951).
[64] Leterrier, Y., Andersons, J., Pitton, Y. and Månson, J.-A. E., *J. Polym. Sci. B: Polym. Phys.* **35**, 1463 (1997).